International Journal of Rock Mechanics & Mining Sciences 46 (2009) 489–497

Contents lists available at ScienceDirect

International Journal of Rock Mechanics & Mining Sciences

journal homepage: www.elsevier.com/locate/ijrmms

Initiation of tensile and mixed-mode fracture in sandstone

Q. Lin [a,*], A. Fakhimi [b,c], M. Haggerty [a], J.F. Labuz [a]

[a] Department of Civil Engineering, University of Minnesota, Minneapolis, MN 55455, USA
[b] Department of Mineral Engineering, New Mexico Tech, Socorro, NM 87801, USA
[c] Department of Civil Engineering, Tarbiat Modarres University, Tehran, Iran

ARTICLE INFO

Article history:
Received 24 March 2008
Received in revised form
28 October 2008
Accepted 31 October 2008

Keywords:
Acoustic emission (AE)
Electronic speckle pattern interferometry (ESPI)
Mixed-mode fracture
Discrete element modeling
Tensile fracture

ABSTRACT

Initiation of failure under three-point bending was observed in sandstone specimens with and without a stress concentrator. Acoustic emission (AE) and electronic speckle pattern interferometry (ESPI) were used to quantify the fracture phenomena through AE locations and ESPI images of an intrinsic damage zone. To investigate mixed mode fracture, beam tests with off-center notches were studied as well. Before about 95% of peak load, the locations of AE were somewhat random for beams with a smooth boundary (no notch). From 96–100% of peak, microcrack hypocenters indicated localization in the form of an intrinsic zone, which was also identified by the high resolution technique of ESPI.

The discrete element technique was used to mimic the failure process. A synthetic rock was composed of rigid circular particles that interact through normal and shear springs, and the particles were glued to each other using normal and shear bonds. A microcrack forming in tension or shear was simulated by breakage of the bond between two particles in contact. The synthetic rock was calibrated for elastic properties, unconfined compressive strength, and bending tensile strength. The beam strength with and without notches and the fracture path were studied in the numerical experiments, and the results compared favorably with those obtained from the laboratory experiments.

1. Introduction

Rock, which can be thought of as a quasi-brittle material because failure is characterized by microcracking, exhibits remarkable behavior when the strength of the material is approached (Fig. 1). For example, in a three-point bending test of a beam composed of Berea sandstone with a smooth boundary (no notch), locations of acoustic emission (AE) up to about 95% of the maximum load indicate that the crack plane is not defined; microcracking is somewhat random (Fig. 1a). The picture is different, however, when the AE hypocenters are determined around peak (Fig. 1b). The localized region, claimed to be an intrinsic property of the material, is clearly identified within a zone approximately 25 mm long and 5 mm wide for this rock, with a grain size of 0.2 mm. After the test, it was observed that the AE locations corresponded to the path of the visible fracture.

The objectives of this research were to (1) study the initiation of failure in smooth-boundary and notched specimens; (2) identify, with improved resolution, the intrinsic zone; (3) model the behavior using a discrete element code. The existence of a localized damage zone prior to fracture in rock was documented by Labuz and Biolzi [1]. This zone is a small volume of rock subjected to distributed microcracking before the appearance of a fracture. Microcracks seem to form somewhat randomly in highly stressed areas prior to failure. Around peak stress, however, microcracks begin to occur in close proximity to the location of the eventual fracture. This clustering continues until a fracture forms and begins to propagate. The damaged volume formed by these microcracks can be thought of as an intrinsic zone, the features of which may be a material property [2].

An experimental technique of exceptional resolution is electronic speckle pattern interferometry called ESPI [3–5], which can be used to observe displacements on the order of microns. ESPI was introduced by Butters and Leendertz [6] and Macovski et al. [7], and is well described by Jones and Wykes [8]. As an optical method, ESPI can obtain high-resolution measurements of surface displacements [9].

The three-point bending test (Fig. 1c) is a simple and useful method to develop a fracture in a laboratory specimen. A smooth boundary (no notch) specimen allows failure to develop without a geometric feature promoting the initiation. The existence of a notch provides a stress raiser to control the development of fracture, either through mode I failure for a center notch beam or mixed-mode failure for an off-center notch beam [10–13]. The discrete element model was used to study the failure pattern observed in the laboratory. The focus of the numerical experiments was on the failure load and the developed damage zone.

* Corresponding author. Tel.: +1 612 6258337.
E-mail address: linx0272@umn.edu (Q. Lin).

1365-1609/$ - see front matter © 2008 Elsevier Ltd. All rights reserved.
doi:10.1016/j.ijrmms.2008.10.008

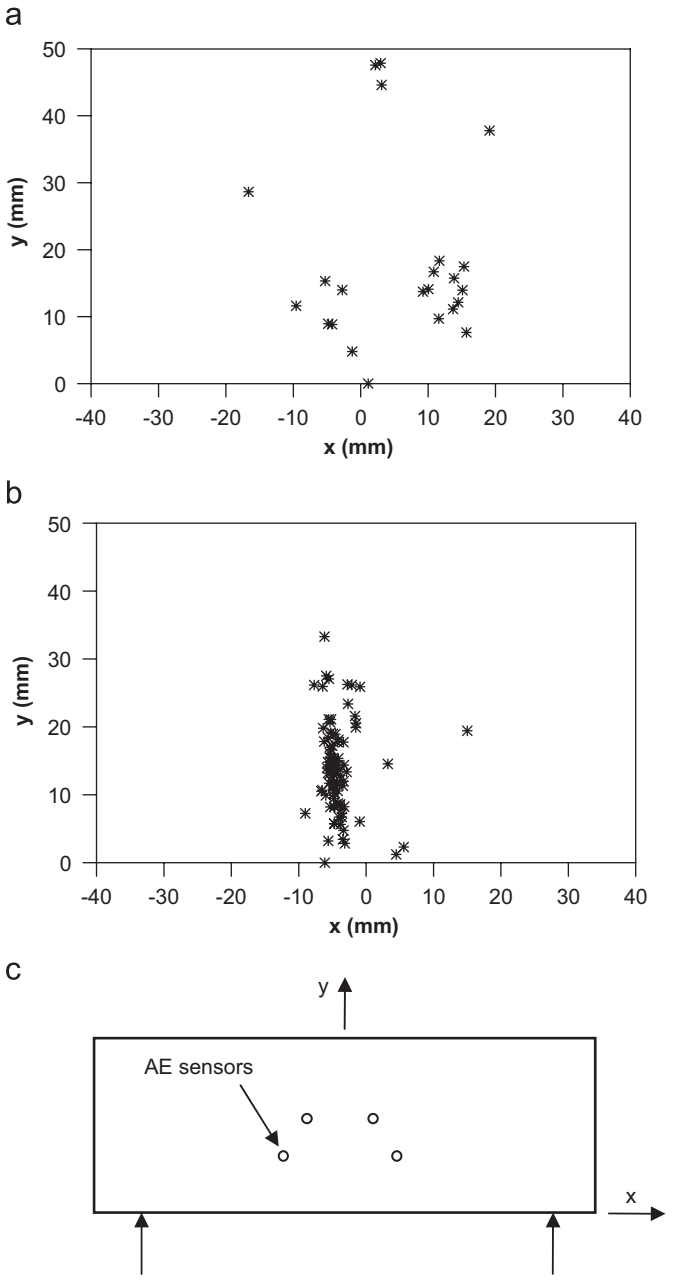

Fig. 1. Three-point bending test with sandstone beam. (a) AE locations pre-localization (up to 95% peak load); (b) AE locations around peak load (98–100%); (c) loading configuration and AE sensor positions.

It is shown that a simple softening contact bond model is capable of simulating the failure process of a quasi-brittle material.

2. Experimental procedure

Berea sandstone was selected for study because of its homogeneous acoustic and optical properties, as well as its fairly uniform grain size. Laboratory testing showed that the Berea sandstone used has a Young's modulus of $E = 10$–12 GPa, a Poisson's ratio of $v = 0.30$–0.35, an unconfined compressive strength of $q_u = 28$–32 MPa, and a bending tensile strength of $\sigma_t = 3.4$–3.6 MPa. Efforts were made to cut all specimens to precise thickness (26.0 mm) and height, although there were some small (0.5 mm) deviations. Two sizes of geometrically similar beams with no notch (a smooth edge) were tested; size 1 spanned 146.8 mm with a 60.0 mm height, whereas size 2 spanned 110.0 mm with a 45.0 mm height. All notched beams had a 60.0 mm height; notch lengths were 10% or 20% of the specimen height (6 or 12 mm). The notch was cut with a water-cooled diamond saw either at one-half the span (the center), or one-third or two-thirds of the half-span length.

A loading system was developed to ensure a steady increase of force with virtually no vibration; this was crucial in the use of ESPI. A disadvantage of the system was the loss of control at maximum load; post-peak response was not captured. A small press (Carver model 17600-77) was used as the load frame, with a hydraulic jack connected to a variable rate pressure system, which consisted of a variable rate motor (Bodine Electric series 400), a gear box (Velmex-UniSlide model B4012BJ), and a pressure generator (High Pressure Equipment model 62610). A 68.95 MPa (10,000 psi) pressure transducer measured the system pressure and the resulting electrical signal was amplified before recording.

2.1. Acoustic emission

The AE system consisted of eight AE sensors (Physical Acoustics model S9225) 3 mm in diameter. Four sensors on one side of the specimen were spaced about 30 mm radially from the notch tip, or beam edge, to allow for laser interferometry imaging. Four AE sensors placed on the other side of the beam were located approximately 25 mm from the notch tip, or beam edge, with one of these selected as the trigger. Each sensor was connected to a preamplifier (Physical Acoustics model 1220C) set to 40 dB gain. The data acquisition system contained four DAQ cards (National Instruments model PCI-5112), each card having two independent channels. A program written with LabView allowed for acquisition of the signals. Once recording was triggered, signals were band-pass filtered (0.1–1.2 MHz) and sampled at 20 MHz over a 200 μs window, with a 100 μs pretrigger. Trigger levels of either 11 or 15 mV were set for each of the tests performed.

Each AE event was recorded as eight waveforms. By determining the arrival time of the *P*-wave in each waveform, it was possible to locate the event coordinates (x,y,z) by minimizing the error between the definition of wave speed (Eq. (1)) and the distance equation (Eq. (2)):

$$d_i = c_P(t_i - t_0) + \varepsilon \tag{1}$$

$$d_i = \sqrt{(x_i - x)^2 + (y_i - y)^2 + (z_i - z)^2} \tag{2}$$

where d_i is the distance from the ith event, c_P the *P*-wave speed of the material, t_0 the time of event, t_i the time recorded from the sensor, ε the error in the measurement (residual), and x_i, y_i, and z_i the coordinates of the ith sensor. The square of the residual is

$$\varepsilon^2 = \sum_{i=1}^{n}([\sqrt{(x_i - x)^2 + (y_i - y)^2 + (z_i - z)^2} + c_P(t_0 - t_i)]^2) \tag{3}$$

The residual was minimized in a least-squares sense using the Levenberg–Marquardt algorithm due to the non-linear nature of Eq. (3).

2.2. ESPI

Electronic (or digital) speckle pattern interferometry involves the analysis of a speckle pattern to obtain information about surface displacements on a specimen. Speckle correlation interferometry infers a comparison between two related speckle images. A speckle pattern is created when monochromatic light